J. Fluid Mech. (1966), *vol.* 26, *part* 2, *pp.* 237–253
Printed in Great Britain

The stability and transition of an axisymmetric wake

By HIROSHI SATO AND OSAMI OKADA
Institute of Space and Aeronautical Science, University of Tokyo, Japan

(Received 2 November 1965)

Experimental and theoretical investigations were made of the instability and transition of the wake behind an axisymmetric slender body at high Reynolds number. The sound from a loudspeaker was used as an artificial disturbance. The velocity fluctuations induced by the sound are selectively amplified depending on the frequency. The wavelength, the phase velocity and the amplification rate of the velocity fluctuations were measured. A linearized stability equation of the disturbance superposed on the axisymmetric wake was solved numerically for both neutral and amplified disturbances. Theoretical results on eigenvalues and eigenfunctions of the stability equation show good agreement with experimental results.

Measurements on phase distributions in streamwise and azimuthal directions indicate that the line of same phase forms a helix and not a series of discrete closed loops.

1. Introduction

In the early stage of the transition from laminar to turbulent flow, a small-amplitude velocity fluctuation is either amplified or damped depending on its wavelength, frequency, etc. This selective amplification has been investigated by a linear theory, using the Orr–Sommerfeld equation. Solutions of the equation were obtained for various flow fields. Experimental verifications of the theoretical results were made for the boundary layer along a flat plate by Schubauer & Skramstad (1948), for the two-dimensional jet by Sato (1959) and for the two-dimensional wake of a thin flat plate placed parallel to a uniform flow by Sato & Kuriki (1961). When the amplitude of the fluctuation exceeds a certain value, non-linear effects become significant. The fluctuation tends to be three-dimensional and the wave-form is distorted. The flow becomes turbulent either by a gradual change of the wave-form of the velocity fluctuations or by a sudden breakdown.

The structure of the three-dimensional wake has long been an interest of many investigators. Marshall & Stanton (1931) observed the wake of a circular disc placed normal to the water flow. The dye trace in the wake showed an unsteady pattern when the Reynolds number based on the disc diameter exceeded about 200. They concluded that there was a periodic discharge from the disc of a series of rings of vortices. The wake of a sphere in a water tank was observed by Möller (1938). From pictures of the flow pattern he found a spiral vortex in the wake in a certain range of Reynolds numbers. Recently, a detailed experiment was made

by Kendal (1963) on the velocity fluctuation in the wake of a sphere in a low-turbulence wind tunnel. From the experimental results on the phase and vorticity distributions, he suggested the existence of a helical vortex filament in the wake when the Reynolds number is of the order of 1000. These experiments are concerned with the wake of bluff bodies. In order to clarify the stability characteristics of the wake, we have to start with a laminar and disturbance-free flow. Bluff bodies usually generate high-level velocity fluctuations.

An analysis of the stability of an axially symmetric jet was made by Batchelor & Gill (1962). They extended the Orr–Sommerfeld equation to the axisymmetric flow and determined a neutral wave-number at an infinite Reynolds number. An experiment of the stability of a circular jet of water into water was made by Viilu (1962), who obtained the minimum critical Reynolds number, based on the diameter and the mean velocity, as about 10. Reynolds (1962) made an experimental investigation of a circular jet and found several modes of instability at Reynolds numbers above 10. In his experiment a spiral pattern of dye was observed when the Reynolds number was around 100. Theoretical and experimental investigations on two-dimensional jets and wakes have shown that the stability characteristics of both flows are very much alike. The objective of the present investigation is to clarify the behaviour of small-amplitude velocity fluctuations in the wake at a relatively high Reynolds number, of the order of 1000. Experimental results are compared with the theoretical results based on the linearized equation of motion.

2. Experimental arrangement

The experiment was conducted in the no. 2 low-turbulence wind-tunnel at the Institute of Space and Aeronautical Science (formerly Aeronautical Research Institute). The tunnel is a non-return type and has test section of 60 by 60 cm cross-section and 300 cm length. The residual turbulence level is around 0·05 % at a flow velocity of 10 m/sec.

In order to investigate the stability of the laminar wake, a slender and sharp-tailed axisymmetric body was placed in the test section parallel to the flow. The body was 30 cm in length and 0·6 cm in maximum diameter, the generatrix approximating a symmetrical aerofoil. The steel body was ground and polished until the surface became like a mirror; the tail tip was made as sharp as a sewing needle. The Reynolds number, based on the free-stream velocity and the diameter of the body, ranged approximately from 1000 to 8000. The shape of the body and the general layout of the test section are shown in figure 1. The cylindrical co-ordinate system (X, r, ϕ) is used, where the origin is at the tail tip of the body, X is the distance measured downstream, and r and ϕ are the radial distances from the axis and the azimuthal angle, respectively.

The body was suspended at two positions by V-shaped fine tungsten wires from the ceiling of the wind tunnel. Since Reynolds number based on the diameter of the suspending wire was about 25 at a flow velocity of 10 m/sec, no shedding of vortex from the wire was expected. Each end of the wires was connected to a screw-gear which was mounted above the ceiling. These four screw-gears were

used for the alignment of the body. For consolidating the parallel setting, a survey of the mean velocity was made in the wake, and the four screw-gears were turned until the velocity distribution became symmetrical in the vertical and horizontal planes. This was actually one of the most tedious tasks in the experiment, for it was found that the alignment must be accurate to within 0·1° in order to realize an axisymmetric wake. Since the symmetricity of the wake was destroyed by the deposit of tiny dust particles on the body, it was carefully cleaned before each experiment.

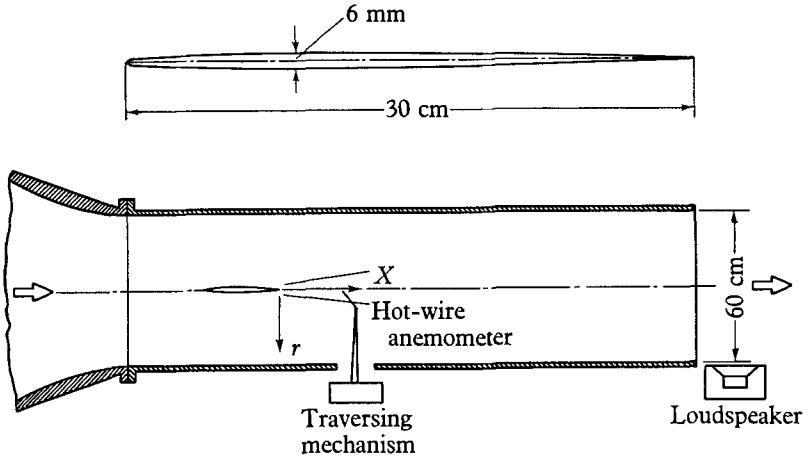

FIGURE 1. Layout of test section. Shape and dimensions of axisymmetric body.

The mean velocity and fluctuation velocity were measured by conventional constant-current hot-wire equipment. The compensated frequency response of the hot-wire and amplifier system was flat from 20 to 10,000 cycles/sec. A 10% rhodium–platinum wire of 0·005 mm diameter was used. The length of the wire was about 1·5 mm. The hot-wire was moved by a D.C. motor in cross-stream and streamwise directions. The position of the hot-wire was transformed into a D.C. voltage by a potentiometer. The accuracy of the positioning was about 0·1 mm. An X–Y recorder was used for recording distributions of various flow quantities. A dual-beam cathode-ray oscilloscope was used for photographic recordings of the wave-form as well as for the measurements of the phase of velocity fluctuations. The spectral components of velocity fluctuations were observed by using a band-pass filter.

The wake of the body was excited artificially by introducing the sound from a loudspeaker into the test section, as shown in figure 1. The intensity of sound was uniform throughout the test section and no resonance effect was observed.

3. Experimental results

The radial distribution of the mean velocity at a flow velocity of 10 m/sec is shown in figure 2. In this case, the wake was artificially excited by the sound of 230 cycles/sec. The excitation was necessary for the experimental results to be reproducible. The transition of a laminar wake is initiated by the residual turbulence in the wind tunnel, and in a low-turbulence tunnel the level of the residual

fluctuation is extremely low and beyond our control. It may be different from one run to another, and this difference was responsible for the poor reproducibility of 'natural transition'. The controlled artificial disturbance improves the reproducibility. The level of the sound was made high enough to mask the residual fluctuations; on the other hand, the intensity of sound must be low enough to

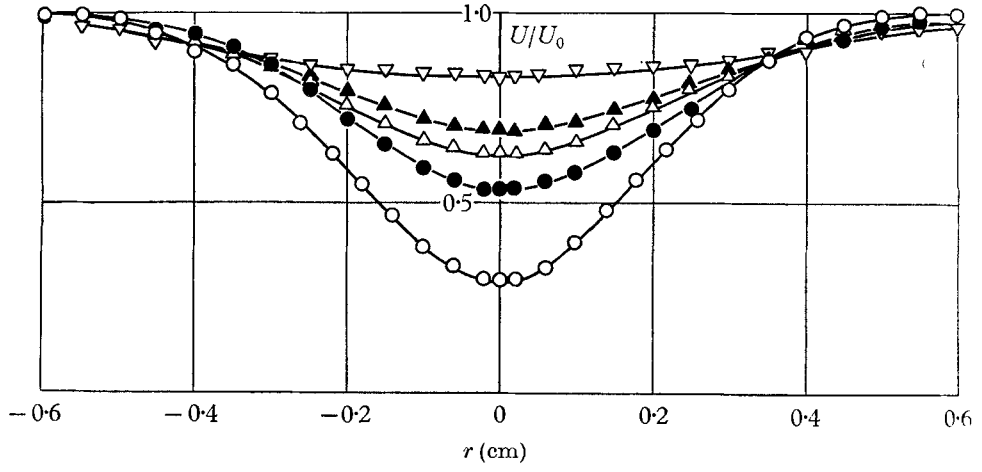

FIGURE 2. Mean-velocity distribution. $U_0 = 10{\cdot}0$ m/sec. ○, $X = 1$ cm; ●, $X = 20$ cm; △, $X = 40$ cm; ▲, $X = 60$ cm; ▽, $X = 100$ cm.

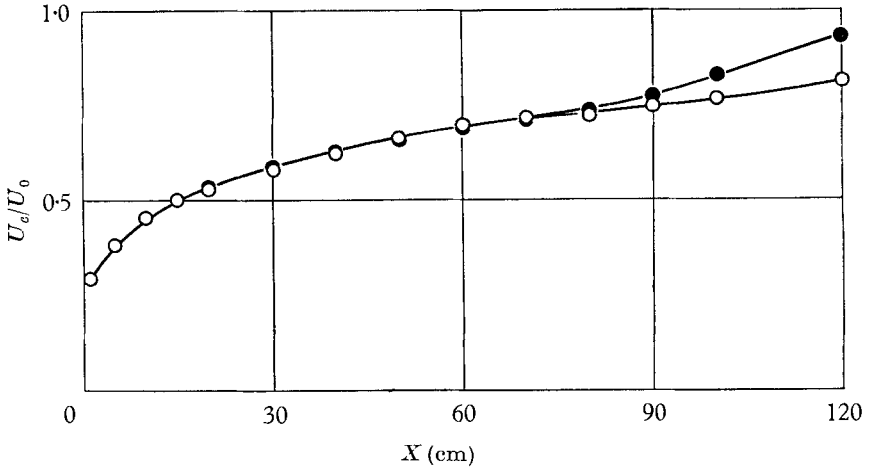

FIGURE 3. Streamwise variation of central velocity U_c. $U_0 = 10{\cdot}0$ m/sec. ○, Without excitation; ●, with excitation, 230 cycles/sec.

avoid disturbing the flow too much. The 230 cycles/sec frequency of exciting sound was chosen to be close to the frequency of fluctuation in the natural transition.

The radius and the central velocity of the wake increase downstream and distribution is almost similar from $X = 20$ to 60 cm. The distribution at $X = 100$ cm is different from others and very flat near the centre line. The streamwise variation of the central velocity U_c non-dimensionalized by the free-stream velocity U_0 and

the half-value radius r_0 non-dimensionalized by the maximum body radius R are shown in figures 3 and 4. The half-value radius is defined as the radius at which the velocity defect is half the maximum defect. Two facts are demonstrated in

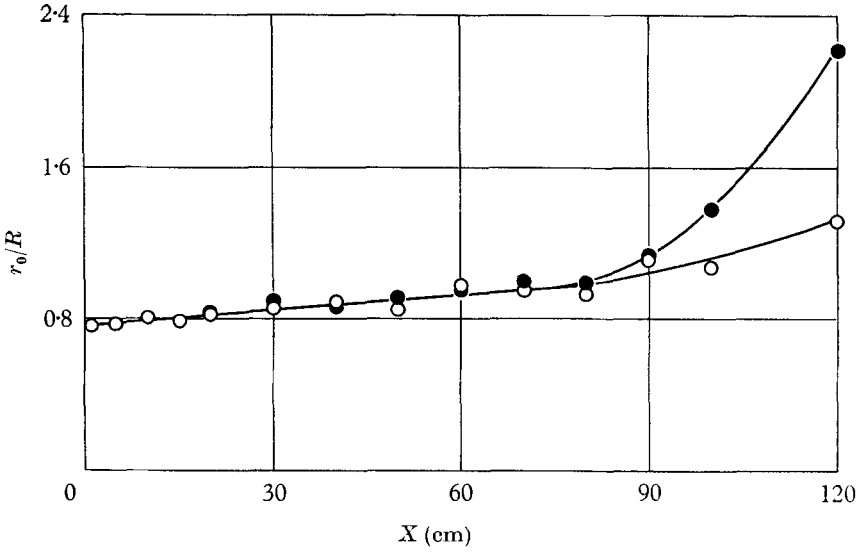

FIGURE 4. Streamwise variation of half-value radius r_0 non-dimensionalized by the maximum radius of the body R. $U_0 = 10{\cdot}0$ m/sec. ○, Without excitation; ●, with excitation, 230 cycles/sec.

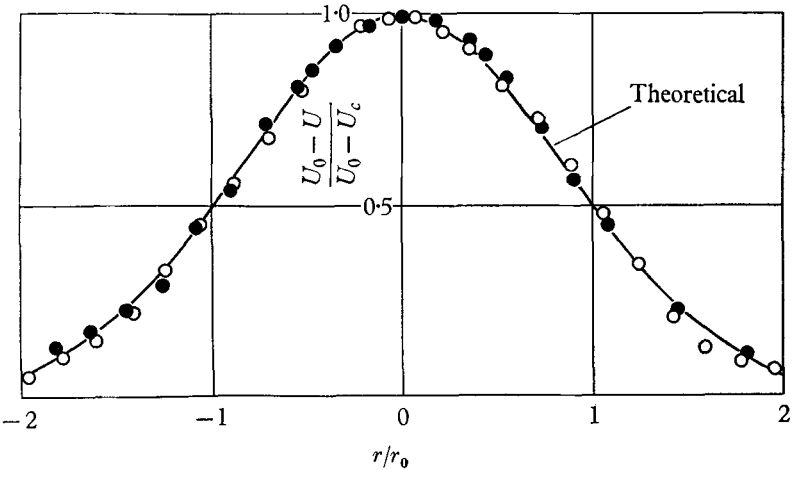

FIGURE 5. Non-dimensional mean-velocity defects. U_c is the velocity on the axis. $U_0 = 10{\cdot}0$ m/sec. ○, $X = 60$ cm; ●, $X = 80$ cm.

the figures. First, both U_c and r_0 do not change much between $X = 20$ and 80 cm. This means that the flow is almost parallel. The radial flow must be very small compared with the axial flow. Secondly, the effect of excitation is small in the region $X < 80$ cm. The central velocity and the half-value radius are not affected by the excitation down to $X = 80$ cm, at which both quantities start increasing rapidly and the laminar-turbulent transition of the wake seems to take place.

The similarity of velocity distribution is demonstrated more clearly in figure 5, in which non-dimensionalized velocity defects at $X = 60$ and 80 cm are plotted.

A velocity distribution given by

$$(U_0 - U)/(U_0 - U_c) = \exp[-a(r/r_0)^2] \tag{1}$$

is shown with a solid line in the same figure. Here, $a\,(= 0{\cdot}69315)$ is a numerical factor for making $(U_0 - U)/(U_0 - U_c) = 0{\cdot}5$ at $r = r_0$. The expression (1) is a solution

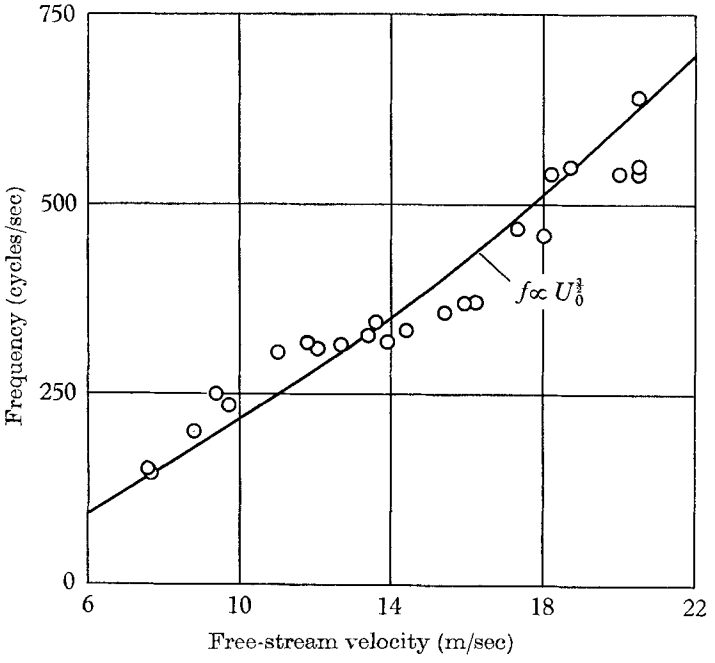

FIGURE 6. Frequency of natural u-fluctuations plotted against free-stream velocity U_0. Solid line indicates $f \propto U_0^{\frac{3}{2}}$.

of the axisymmetric laminar-boundary-layer equation applied for the wake. In the equation the momentum defect is assumed constant in the axial direction and $(U_0 - U)^2$ is neglected in comparison with U_0^2. The agreement with experimental results is fairly good.

When the free-stream velocity exceeds about 8 m/sec, velocity fluctuations with almost sinusoidal wave-form appear in the wake. The dominant frequency of the observed fluctuations in the natural transition is plotted against the free-stream velocity in figure 6. It is difficult to measure the frequency accurately because the frequency itself seems to fluctuate. Data shown in the figure are values averaged over several minutes. A simple dimensional analysis suggests that the frequency might be proportional to U_0/r_0. Since the half-value radius r_0 is nearly proportional to $1/\sqrt{U_0}$, the frequency might be roughly proportional to the $\frac{3}{2}$ power of the free-stream velocity. The solid line in the figure indicates this relation and experimental points lie near the line.

In figure 7 is shown a map of the fluctuation patterns at a free-stream velocity of 10 m/sec with the exciting sound of 230 cycles/sec. The radial distance is

enlarged for clear illustration. It is impossible to draw a map in the case of no excitation because the fluctuation field is not reproducible from one run to another. The wave-forms of the fluctuations taken at various positions in the flow field are shown in the figure. The wake is laminar to start with; there is no velocity fluctuation between $X = 0$ and 20 cm. The velocity fluctuation with sinusoidal wave-form first appears at about $X = 20$ cm in the off-axis region. At

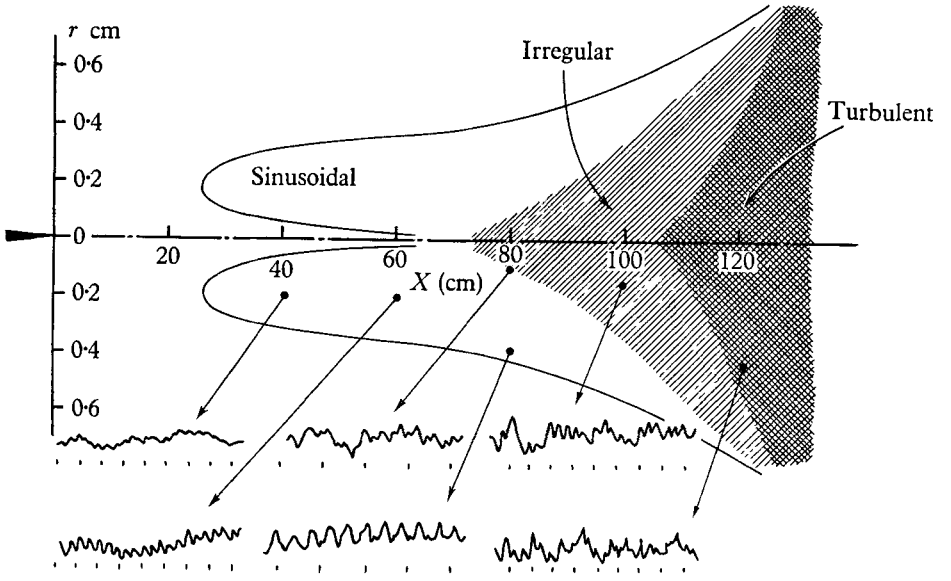

FIGURE 7. Map of fluctuation patterns and oscillographic records of u-fluctuations. $U_0 = 10{\cdot}0$ m/sec. Time, from left to right, and the interval between dots, 10 msec.

about $X = 70$ cm the wave-forms near the axis become irregular. For $X > 80$ cm the region of irregular fluctuation expands very rapidly. The second harmonic fluctuation, namely the fluctuation with doubled frequency of exciting sound, is sometimes observed near the axis. The intensity of this fluctuation is far smaller than that of the fundamental component. A detailed observation shows that the second harmonic fluctuation increases when the body has an angle of attack to the flow. As mentioned earlier, the body was carefully aligned to the free stream, and when the alignment was considered to be perfect, the second harmonic fluctuation was extremely small.

Radial distributions of the root-mean-square value of the fluctuating velocity with the excitation are shown in figure 8. The intensity reaches the maximum at about $X = 100$ cm. There is a remarkable increase on the axis from $X = 80$ cm to $X = 100$ cm. This may be related to the increases of irregular fluctuation near the axis shown in figure 7.

Using a band-pass filter which was tuned to the frequency of the exciting sound, measurements were made of the amplitude and phase of the spectral components. Distributions of the amplitude of the spectral component of 230 cycles/sec are shown in figure 9. All distributions including those at $X = 100$ and 120 cm show two distinct peaks and become nearly zero on the axis. Com-

parison of figures 8 and 9 indicates clearly that the irregular velocity fluctuations contribute to the large value of $(\overline{u^2})^{\frac{1}{2}}$ on the axis at large X. Peaks in the distributions of the spectral component are located at about the radii of the maximum $\partial U/\partial r$. At $X = 120$ cm peaks are found considerably further from the axis. This fact is consistent with the rapid widening of the wake at large X shown in

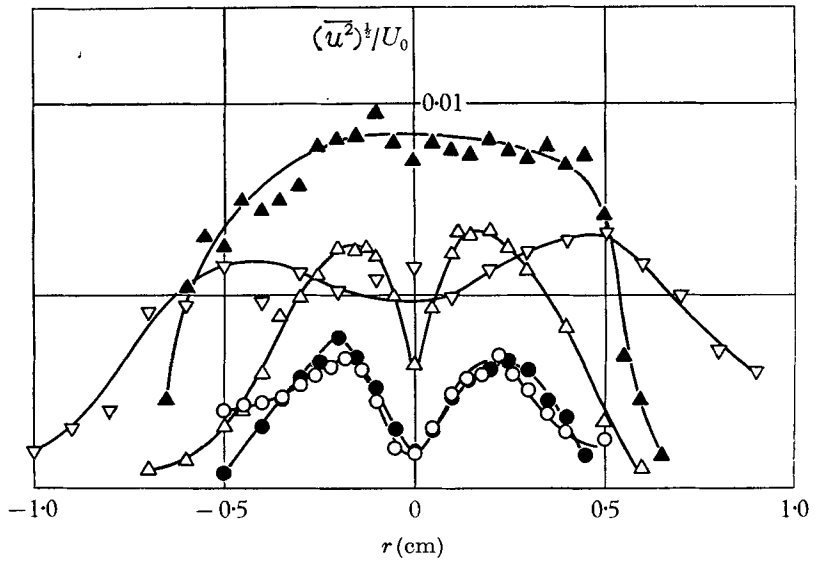

FIGURE 8. Radial distribution of intensity of u-fluctuations. Excitation, 230 cycles/sec. $U_0 = 10{\cdot}0$ m/sec. ○, $X = 40$ cm; ●, $X = 60$ cm; △, $X = 80$ cm; ▲, $X = 100$ cm; ▽, $X = 120$ cm.

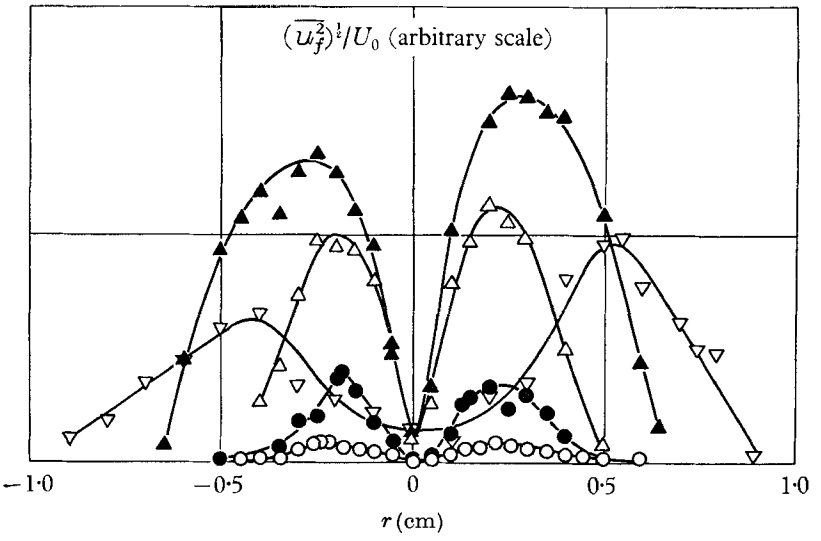

FIGURE 9. Radial distribution of the amplitude of the spectral component. The ordinate is in arbitrary scale, while the r lative values at various X-stations are shown correctly. Excitation, 230 cycles/sec, $U_0 = 10{\cdot}0$ m/sec. ○, $X = 40$ cm; ●, $X = 60$ cm; △, $X = 80$ cm; ▲, $X = 100$ cm; ▽, $X = 120$ cm.

figure 4. Streamwise variations of the maximum values of the amplitude of the excited spectral components at each X-station $(\overline{u_f^2})^{\frac{1}{2}}_{\max}$ are shown in figure 10 in a semi-logarithmic plot. The band-pass filter was tuned to the frequency of the exciting sound which was varied from 175 to 425 cycles/sec. In the region $X < 80$ cm, the amplitude increases exponentially with X. The spatial amplification rate is given by a gradient of each straight line. The gradient is different for different frequencies. The overall velocity fluctuation $(\overline{u^2})^{\frac{1}{2}}$ does not grow exponentially in the X-direction since this fluctuation is the sum of various spectral components which are amplified with different amplification rates corresponding to their frequencies.

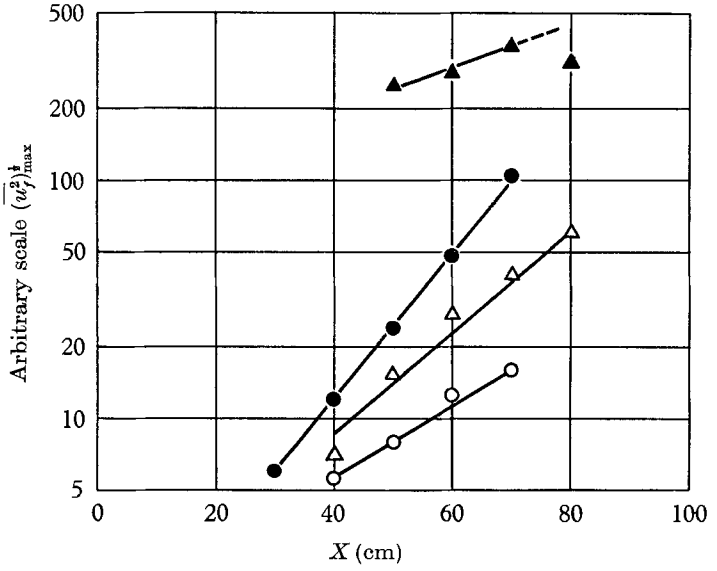

FIGURE 10. Streamwise growth of spectral components. $U_0 = 10{\cdot}0$ m/sec. The ordinate scale is arbitrary. Excitation: ○, 175 cycles/sec; ●, 230 cycles/sec; △, 325 cycles/sec; ▲, 425 cycles/sec.

Phase relations of velocity fluctuations were observed in azimuthal, radial and axial directions by taking the correlation with a standard signal. The sound from the loudspeaker was used as the phase standard because the sound had a definite phase relation with the induced velocity fluctuation. Experimental results indicate that the phase of velocity fluctuation changes in azimuthal, radial and streamwise directions. As is shown in figure 11, the phase at the constant radius varies almost linearly with the azimuthal angle and changes 360° for one turn. Since the phase changes linearly also with the streamwise direction, the line of the same phase is a helix and not a closed loop. This fact suggests the existence of a helical vortex system in the wake. However, this cannot be stated with confidence because vorticity measurements have not been made so far. The radial phase distribution is shown in figure 12. The phase difference at any two symmetrical points with respect to the axis is almost 180° and the phase jumps about 180° on the axis. The streamwise distribution of the phase is shown in figure 13. The phase angle changes linearly in the streamwise direction. The

period of the phase distribution gives the wavelength of the velocity fluctuation. The wavelength, the spatial amplification and the distributions of the amplitude and phase are to be compared with theoretical results in a later section.

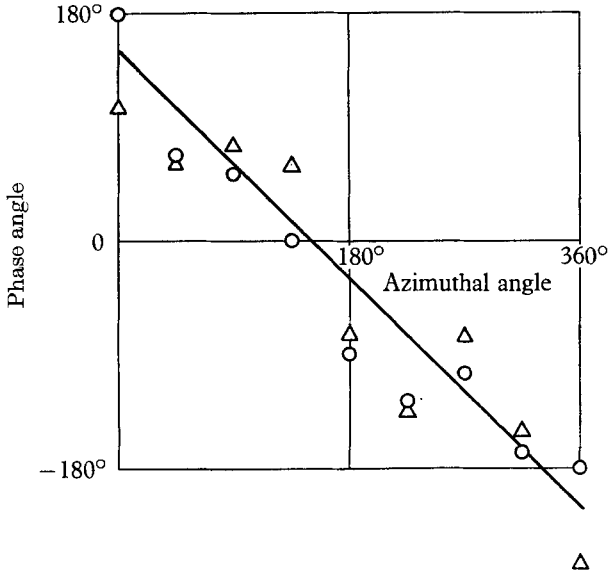

FIGURE 11. Azimuthal distribution of the phase of velocity fluctuation. Excitation 230 cycles/sec. $U_0 = 10{\cdot}0$ m/sec. ○, $X = 40$ cm, $r = 0{\cdot}24$ cm; △, $X = 80$ cm, $r = 0{\cdot}26$ cm.

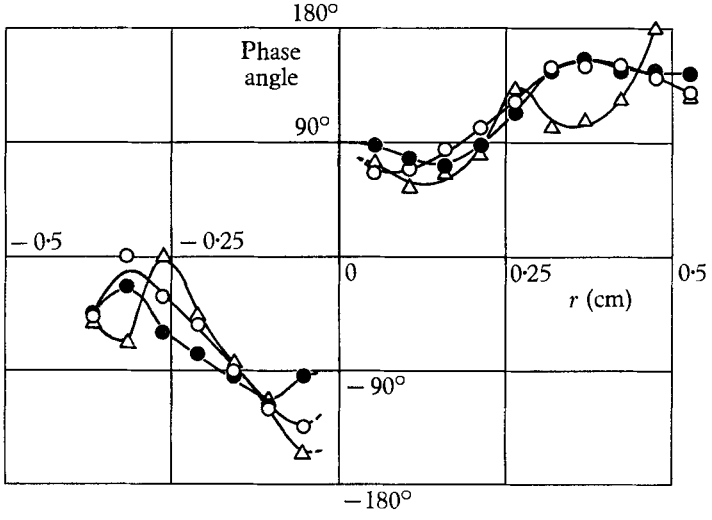

FIGURE 12. Radial distribution of the phase of the spectral component. Excitation 230 cycles/sec. $U_0 = 10{\cdot}0$ m/sec. ○, $X = 60$ cm; ●, $X = 70$ cm; △, $X = 80$ cm.

4. Stability theory of an axisymmetric wake

Theoretical investigations of the stability of axisymmetric free boundary layers such as jets and wakes are rather scanty compared with those of two-dimensional flow. Batchelor & Gill (1962) made an analysis of the stability of an

axisymmetric jet. They investigated fundamental features of the stability of axisymmetric free layers in general. They showed a necessary condition for the existence of neutral oscillations and calculated a neutral wave-number of jet at an infinite Reynolds number. The stability characteristics of jets and wakes are very much alike. Gold (1964), in his investigations of the stability of jets and wakes of compressible fluid, extended the condition given by Batchelor & Gill to the compressible flow. In order to compare the experimental results with stability theory, however, one has to calculate not only the neutral disturbance but also amplified disturbances. We follow the same procedure used by Batchelor & Gill and calculate the amplified disturbances numerically.

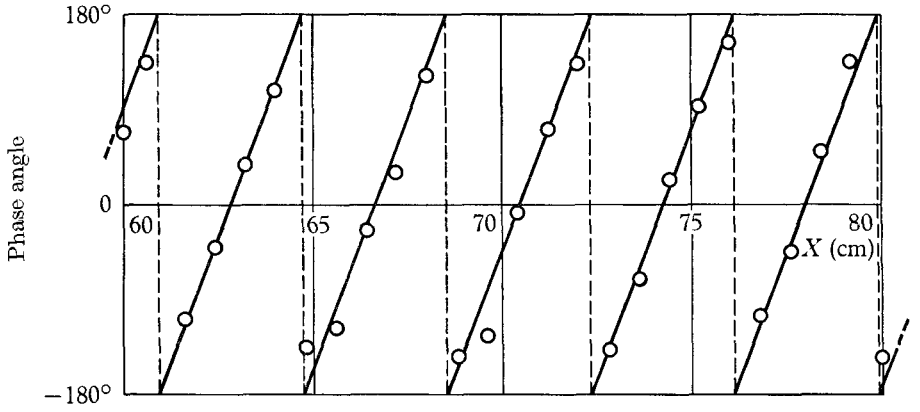

FIGURE 13. Streamwise distribution of the phase of the spectral component. Excitation 230 cycles/sec. $U_0 = 10{\cdot}0$ m/sec. $r = 0{\cdot}3$ cm.

The flow is assumed to be incompressible and inviscid. It is known that the stability characteristics of free boundary layers do not depend on the Reynolds number when the Reynolds number is large. The critical Reynolds number of the axisymmetric jet seems to be, according to the experiment of Reynolds (1962), less than 300. In the present experiment the Reynolds number based on the diameter of the body and the free-stream velocity is around 4000, which seems to be large enough to make the viscosity effect negligible in the stability calculation.

The linearized equation is derived from the Navier–Stokes equation by the conventional procedure. The flow quantities are non-dimensionalized by the free-stream velocity U_0 and the half-value radius r_0. The mean flow is assumed to be axisymmetric and parallel. The following linearized equations are obtained for the disturbance velocities u_x, u_r, u_ϕ and pressure p in non-dimensional forms:

$$\left.\begin{aligned} \frac{\partial u_x}{\partial t} + U(r)\frac{\partial u_x}{\partial x} + u_r\frac{\partial U(r)}{\partial r} &= -\frac{\partial p}{\partial x}, \\ \frac{\partial u_r}{\partial t} + U(r)\frac{\partial u_r}{\partial x} &= -\frac{\partial p}{\partial r}, \\ \frac{\partial u_\phi}{\partial t} + U(r)\frac{\partial u_\phi}{\partial x} &= -\frac{1}{r}\frac{\partial p}{\partial \phi}, \end{aligned}\right\} \tag{2}$$

$$\frac{\partial u_x}{\partial x}+\frac{1}{r}\frac{\partial (ru_r)}{\partial r}+\frac{1}{r}\frac{\partial u_\phi}{\partial \phi}=0, \tag{3}$$

in which $U(r)$ is the mean velocity and p is non-dimensionalized by ρU_0^2.

Fluctuating components are resolved into Fourier components of the form

$$\left.\begin{aligned} u_x &= \mathrm{Re}\,[F(r)\exp\{in\phi+i\alpha(x-ct)\}],\\ u_r &= \mathrm{Re}\,[iG(r)\exp\{in\phi+i\alpha(x-ct)\}],\\ u_\phi &= \mathrm{Re}\,[H(r)\exp\{in\phi+i\alpha(x-ct)\}],\\ p &= \mathrm{Re}\,[P(r)\exp\{in\phi+i\alpha(x-ct)\}], \end{aligned}\right\} \tag{4}$$

where F, G, H and P are complex amplitude functions, α is the wave-number and $c=c_r+ic_i$ is the complex wave velocity. Since the phase angle between u_x and u_r is 90° as shown in equation (3), we put $u_r \propto iG$. The periodicity of the fluctuation with respect to the azimuthal angle ϕ is given by an integer n. When $n=0$, the velocity fluctuation is axially symmetric; in other words, the phase does not change in the azimuthal direction. When $n=1$, the fluctuation is in the sinuous mode. The phase angle of this mode varies linearly in the azimuthal direction and changes 360° for one turn around an axis. The phase of the fluctuation with $n=2$ changes 720° for one turn.

On substituting (4) in equations (2) and (3) we obtain

$$\alpha(U-c)F+U'G=-\alpha P, \tag{5}$$

$$\alpha(U-c)G=P', \tag{6}$$

$$\alpha(U-c)H=(n/r)P, \tag{7}$$

$$\alpha F+G'+(G/r)+(n/r)H=0, \tag{8}$$

in which a prime denotes differentiation with respect to r. By eliminating F, H and P from equations (5) to (8), we obtain a single equation as to G,

$$(U-c)\frac{d}{dr}\left\{\frac{r}{n^2+\alpha^2r^2}\frac{d}{dr}(rG)\right\}-(U-c)G-rG\frac{d}{dr}\left(\frac{rU'}{n^2+\alpha^2r^2}\right)=0. \tag{9}$$

Boundary conditions are given on the axis and at infinity. The conditions to be satisfied at infinity are simply that the amplitude functions F, G, H and P tend to zero as $r\to\infty$. The conditions on the axis are found from equations (5) to (8). Conditions on the axis for $n=0$ are

$$\left.\begin{aligned} &F, P\text{: finite},\\ &G=H=0 \quad \text{at} \quad r=0. \end{aligned}\right\} \tag{10}$$

Conditions for $n=1$ are

$$\left.\begin{aligned} &F=P=0,\\ &G=-H\text{: finite} \quad \text{at} \quad r=0. \end{aligned}\right\} \tag{11}$$

Conditions for $n=2$ are

$$F=G=H=P=0 \quad \text{at} \quad r=0. \tag{12}$$

Detailed discussions on boundary conditions are found in the paper by Batchelor & Gill (1962).

From equation (9), the following expression is obtained when $c_i = 0$,

$$r\frac{d}{dr}\left\{\frac{r}{1+(\alpha^2r^2/n^2)}\frac{d}{dr}(rG)\right\} = \left\{n^2-\frac{r}{c_r-U}\frac{d}{dr}\left(\frac{rU'}{1+(\alpha^2r^2/n^2)}\right)\right\}rG. \tag{13}$$

From this equation Batchelor & Gill derived a criterion that gives a necessary condition for the existence of the neutrally stable disturbance. They applied the criterion for an axisymmetric jet with a velocity distribution given by

$$U = 1/(1+r^2)^2, \tag{14}$$

and concluded that the disturbance with $\alpha \neq 0$ can exist only for $n = 1$. They actually obtained a solution for $n = 1$ by numerical integrations.

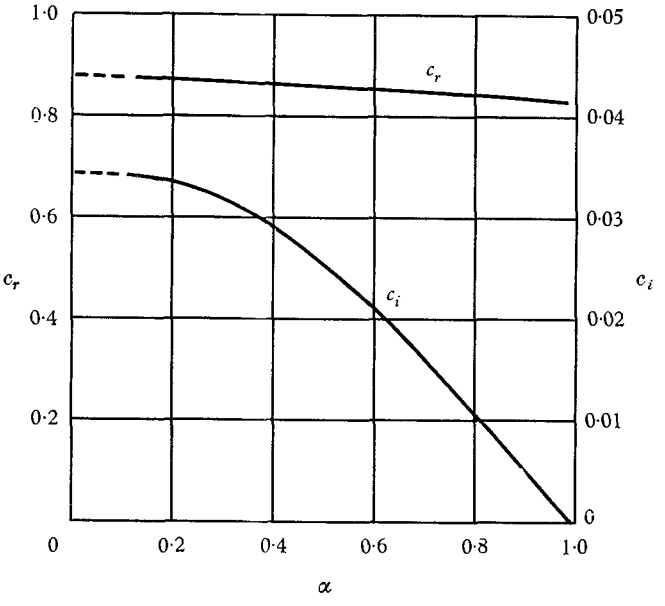

FIGURE 14. Theoretical results on the rate of amplification and the propagation velocity. Amplified disturbance for mode $n = 1$.

In the present calculation the velocity distribution (1) was used because it fits better than (14) to experimental results. In the non-dimensional form U is expressed as

$$U = 1-q\exp(-ar^2), \tag{15}$$

in which $a = 0{\cdot}69315$ and q is the maximum value of the velocity defect. Considering experimental results, we take $q = 0{\cdot}3$. For the velocity distribution such as (15) unstable fluctuations are excluded for $n = 0$ as pointed out by Batchelor & Gill. We used Batchelor & Gill's criterion for this velocity distribution and found that the solutions for neutral disturbance may exist only for $n = 1$ and $n = 2$. Numerical integrations for the neutral disturbance were made for both values of n. A solution was obtained only for $n = 1$ and no solution was obtained for $n = 2$. This is not surprising, because the condition given above is a necessary condition but not a sufficient one. Gold (1964) made an analysis of the stability

of the compressible axially symmetric wake and concluded that the sinuous mode is the most unstable one. According to his description, the instability of a sinuous mode is closely related to the fact that the radial component of disturbance is allowed to exist on the axis.

Numerical calculations for the amplified disturbances were performed for $n = 1$ by the Runge–Kutta procedure using an OKITAC 5090 electronic computer. Eigenvalues of c_i and c_r are obtained as functions of the wave-number α as shown in figure 14. The maximum value of the amplification rate αc_i is 0·0126 at $\alpha = 0{\cdot}54$ and $c_r = 0{\cdot}852$ and the maximum value of the spatial amplification rate $\alpha c_i/c_r$ is 0·0148 at $\alpha = 0{\cdot}55$ and $c_r = 0{\cdot}851$. Computed results on distributions of amplitude and phase of amplified fluctuations are to be compared with the experimental results in the following section.

5. Discussion

In the process of experimental investigation two facts became clear. One is the poor reproducibility of the so-called natural transition. The transition of the wake behind a streamlined body can be initiated by the residual turbulence in the wind tunnel, because the disturbance generated by the body is extremely small, and since the intensity and the frequency spectrum of the turbulence may not be the same for each experimental run, reproducibility is not assured. The introduction of an artificial disturbance is essential for studying the stability of free boundary layers such as jets and wakes. The other fact is the effect of tiny dust particles on the body. When the dust deposits on the body, the fluctuation in the wake increases and the velocity defect recovers very rapidly. Moreover, since the dust deposits only on the upper surface of the body, the axisymmetry of the wake is destroyed.

The wake of an axisymmetric streamlined body is divided into four regions: the laminar, the linear, the non-linear and the turbulent regions.

The laminar region in the present experiment extends about 20 cm from the tail tip of the body. The boundary layer on the solid body is laminar. After the boundary layer separates at the tail tip it rearranges itself to form a laminar axisymmetric wake. The increase of the velocity on the axis is remarkable. At about $X = 20$ cm the mean-velocity distribution settles into a similar distribution. When the disturbance in the flow is small, it grows after the wake becomes similar. On the other hand, if the disturbance is large, it is expected that the disturbance grows in the non-equilibrium region of the wake. The latter is the case for the wake of a blunt body.

The linear region follows the laminar region and extends from $X = 20$ to about 70 cm, in which the spectral component of the velocity fluctuation grows exponentially downstream. In this region the flow field is approximately parallel and the mean velocity distribution is kept almost unchanged. The radial distribution of the intensity of the velocity fluctuation has two peaks and shows a small value on the axis. The experimental results at $U_0 = 10$ m/sec and $X = 60$ cm are compared with the theoretical results of the mode $n = 1$ in figures 15, 16 and 17. Eigenvalues are compared in figure 15. The wave-number α plotted against the

frequency αc_r shows a good agreement. The non-dimensional frequency corresponding to the neutral disturbance is 0·820. Concerning the amplification rate a time-space transformation is necessary. In the stability theory the disturbance

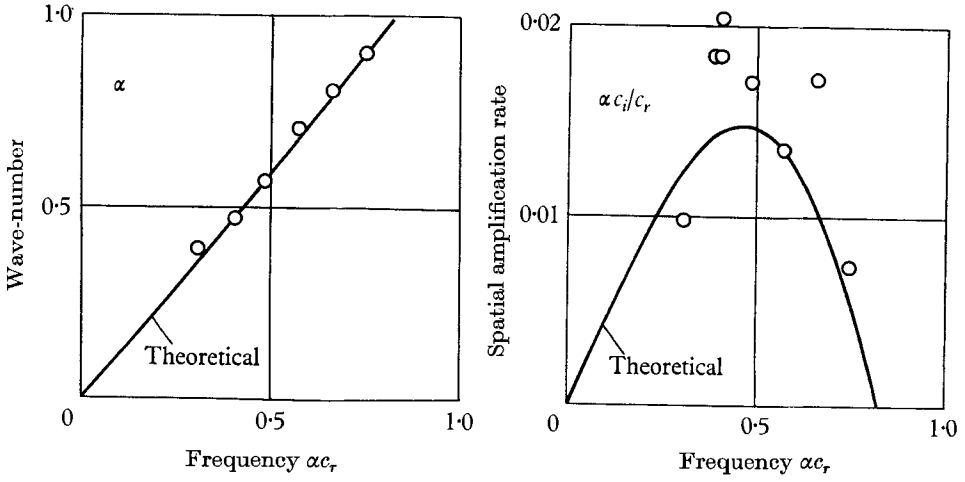

FIGURE 15. Wave-number α and spatial rate of amplification $\alpha c_i/c_r$ against non-dimensional frequency αc_r.

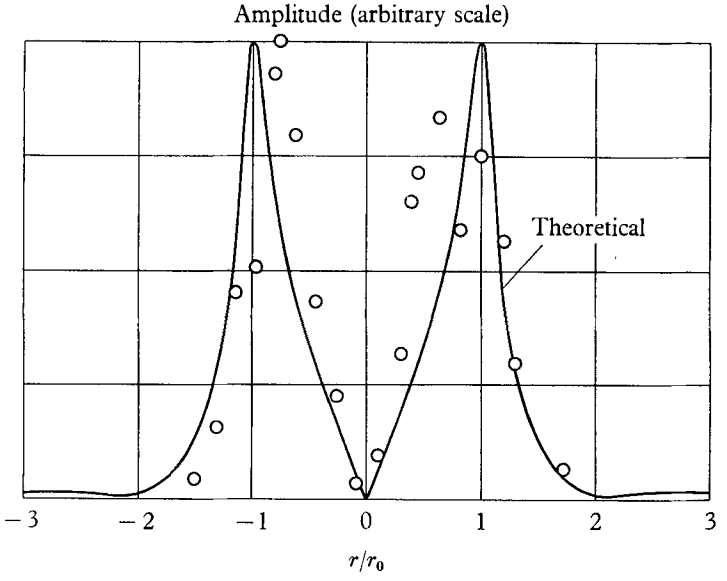

FIGURE 16. Amplitude function of amplified fluctuation. ○, Experimental results at $X = 60$ cm. In theoretical results $\alpha = 0{\cdot}475$ and $c_i = 0{\cdot}026$

is amplified as a function of time. In the experiment, however, the disturbance is amplified in the direction of flow, with the spatial amplification rate $\alpha c_i/c_r$. The agreement between the theory and the experiment is fairly good but not as good as that with the wave-number. In figures 16 and 17 the amplitude and the phase are compared. Theoretical curves in both figures are for eigenvalues corresponding

to experimental conditions. The agreement is, in general, good. In the experiment a 180° phase-jump at about $r/r_0 = 2$ is not observed. As shown in the amplitude distribution, the amplitude around $r/r_0 = 2$ is very small and the phase could not be measured. The phase changes linearly in the azimuthal direction. These experimental and numerical results indicate that the behaviour of a small-amplitude velocity fluctuation in this region is explained by the linearized stability theory and that in the axisymmetric wake the velocity fluctuation of the mode $n = 1$ exists.

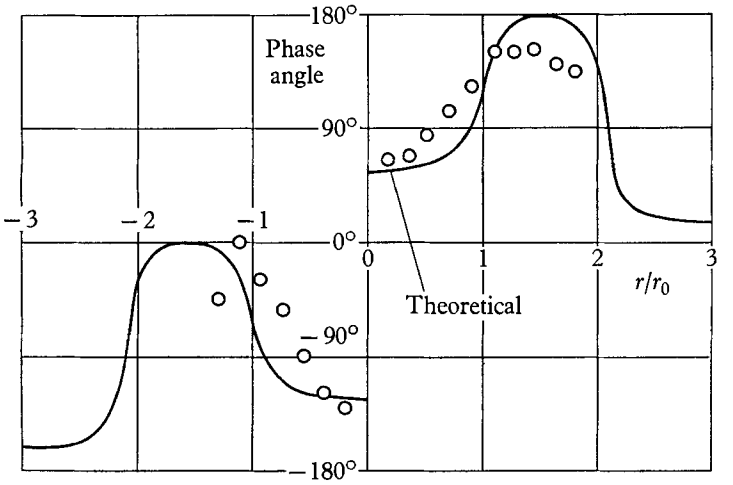

FIGURE 17. Radial phase distribution of amplified fluctuation. ○, Experimental results at $X = 60$ cm. In theoretical results $\alpha = 0{\cdot}475$ and $c_i = 0{\cdot}026$.

The non-linear region then extends downstream. The amplification rate of the velocity fluctuations is no longer exponential. While velocity fluctuations lose their regular periodicity, still the wave-form is not completely irregular. The half-value radius and the central velocity start increasing very rapidly. This implies the action of Reynolds stress on the mean velocity. The production of a velocity fluctuation due to the non-linear effect causes the increase of irregular components, especially near the axis. In figure 8 a remarkable increase of the intensity of fluctuation at $X = 100$ cm is illustrated. The non-linear region is followed by the turbulent region in which no periodicity is found in the wave-form of fluctuation. No detailed measurements were made in this region.

There is an important difference between the two-dimensional and the axisymmetric wakes in the second-harmonic fluctuation, that is, the fluctuation with the doubled frequency. The second-harmonic fluctuation was clearly observed in the two-dimensional wake of a thin flat plate (Sato & Kuriki 1961) and in the wake of a circular cylinder (Roshko 1953). The transverse phase distribution of the second-harmonic fluctuation was symmetric with respect to the central plane. On the other hand, the second-harmonic component was observed in the axisymmetric wake only when the body had an angle of attack. The component was observed near the axis but the distribution of the amplitude was not axisymmetric.

6. Conclusion

The experimental and theoretical investigations of the axisymmetric wake behind a stream-lined slender body indicate that the wake is classified into four regions, which are the laminar, linear, non-linear and turbulent regions. In the laminar regions the separated laminar boundary layer develops into the laminar wake. In the linear region the mean-velocity distribution is kept almost unchanged and the flow is almost parallel. Small-amplitude velocity fluctuations in a certain frequency range are amplified as they travel downstream. The measured wavelength, amplification rate and distribution of the amplitude and phase are in good agreement with the results of linearized theory. The phase measurements in azimuthal and axial directions indicate that the line of the same phase forms a helix and not discrete loops. In the non-linear region the production of an irregular velocity fluctuation is observed but the second-harmonic component is not found. The regularity in the wave-form of fluctuation is gradually lost in the non-linear region. The turbulent region is established without any bursts or sudden breakdown.

The authors wish to express their gratitude to Professor Itiro Tani and Dr J. M. Kendall for their valuable suggestions, and to members of the Boundary Layer Research Group in Japan for their stimulating discussions. Thanks are extended to Messrs Y. Onda and S. Korenaga who helped to carry out the experimental work.

REFERENCES

BATCHELOR, G. K. & GILL, A. E. 1962 *J. Fluid Mech.* **14**, 529.

GOLD, H. 1964 Private communication.

KENDALL, J. M. 1963 Private communication.

MARSHALL, D. & STANTON, T. E. 1931 *Proc. Roy. Soc.* A, **130**, 295.

MÖLLER, W. 1938 *Phys. Zeit.* **39**, 57.

REYNOLDS, A. J. 1962 *J. Fluid Mech.* **14**, 552.

ROSHKO, A. 1953 *Nat. Adv. Comm. Aero., Wash. TN* no. 2913.

SATO, H. 1959 *J. Fluid Mech.* **7**, 53.

SATO, H. & KURIKI, K. 1961 *J. Fluid Mech.* **11**, 321.

SCHUBAUER, G. B. & SKRAMSTAD, H. K. 1948 *Nat. Adv. Comm. Aero., Wash., Rep.* no. 909.

VIILU, A. 1962 *J. Appl. Mech.* **29**, 506.